Analysis of the Mixing Conditions of a Toner Dispersion*

H. Göktürk† *, K. Suenaga, M. Yamazaki, S. Moriyama*

Kao Corporation, Recording and Imaging Science Laboratory, 1334 Minato, Wakayama 640, Japan

Abstract

Twin screw extruder mixing of a typical black toner formulation was investigated under different mixing conditions. The intensity of the mixing was varied by changing the feed rate of the material and the screw rpm of the extruder. Microstructural changes in the particulate fillers were analyzed by transmission electron microscopy. The fillers were characterized in terms of their particle size and shape distributions and spatial distributions within the binder. Changes in the molecular structure of the binder polymer were identified by gel permeation chromatography and softening temperature measurements. Temperature-variable dielectric properties and rheological properties of the bulk material samples were investigated as possible tools for understanding the degree of dispersion. Results indicate that both methods are sensitive to the changes introduced by different processing conditions. Charging properties of the pulverized samples were also characterized. Both charge per unit mass values and charge distributions of the toner particles were found to be adversely influenced by increasing intensity of mixing.

Introduction

Preparation of the toner dispersion involves a number of challenges in terms of the mixing process. The filler particles added to the polymer are usually in the form of aggregates which must be broken down into primary particles. Then the particles must be distributed within the binder homogeneously. To maintain the physical properties desirable for the toner, neither intensive nor extensive mixing should alter the binder microstructure significantly. Proper selection of the mixing conditions to satisfy these somewhat conflicting requirements is the primary motivation of this study.

One of the prevalent methods of preparing the toner dispersion is mixing in a twin screw extruder.[1] Twin-screw extruders consist of flexible mixing elements that can be arranged in a multitude of combinations so as to perform different tasks.[2,3] The variety of combinations available also makes the operation of this mixer somewhat complicated. Twin-screw extrusion, when employed, serves as the main mixing step in the preparation of the toner dispersion and influences the ultimate properties of the toner significantly.

The toner dispersion is usually evaluated after the pulverization of the processed material by measuring the charging and printing properties of the surface-treated powder.[4–7] Although measurement of these properties is very important, the evaluation is somewhat removed from the mixing step, and measured properties are difficult to relate to the process parameters. Evaluation of the quality of the dispersion right after or, preferably, during the mixing is more desirable to understand and to control the mixing process well.

Objectives of the study are to investigate the influence of different mixing conditions on the state of a toner dispersion and to develop new tools that could be used to evaluate the degree of dispersion. Special consideration is given to evaluation methods that are promising for on-line implementation.

Table I. Formulation of the Toner

	Material	Parts by wt.
Toner binder	Polyester resin	100
Main filler	Carbon black	6
Charge control agent	Organic pigment	1
Magnetic filler	Magnetite	3
Wax	Polypropylene	3

Experimental

The formulation given in Table I represents a typical black toner. The binder is a polyester resin of average molecular weight 66,000, glass transition temperature 67°C, softening temperature 132°C, and gel content 20%. Carbon black specifications are surface area 138 m^2/g, primary particle size 24 nm, and oil (dibutyl phthalate) absorption 60 cm^3 per 100 g. The wax is a homopolymer of polypropylene with a melting temperature of 135 to 144°C. The charge control agent (CCA) is chrome azobenzene complex. The magnetite has an average particle size of 260 nm and surface area of 7 m^2/g.

The materials were premixed in a batch mixer; then the premix was fed to a corotating, intermeshing twin-screw extruder for further processing. Four different mixing conditions were created by varying the feed rate and the screw rpm as listed in Table II. At each setting of the rpm and feed rate, material samples were collected after the mixing had reached a steady state as observed by the gauges. The mixing process was monitored by measuring the screw rpm, the power expended by the mixer, the melt temperature, and the feed rate. Specific energy consumption, i.e., the energy imparted by the extruder to unit mass of the material, is used as a measure of the mixing intensity[8]:

$$\text{Specific energy} = \frac{(P - P_0) \times \text{Efficiency}}{\text{Feed rate}}, \qquad (1)$$

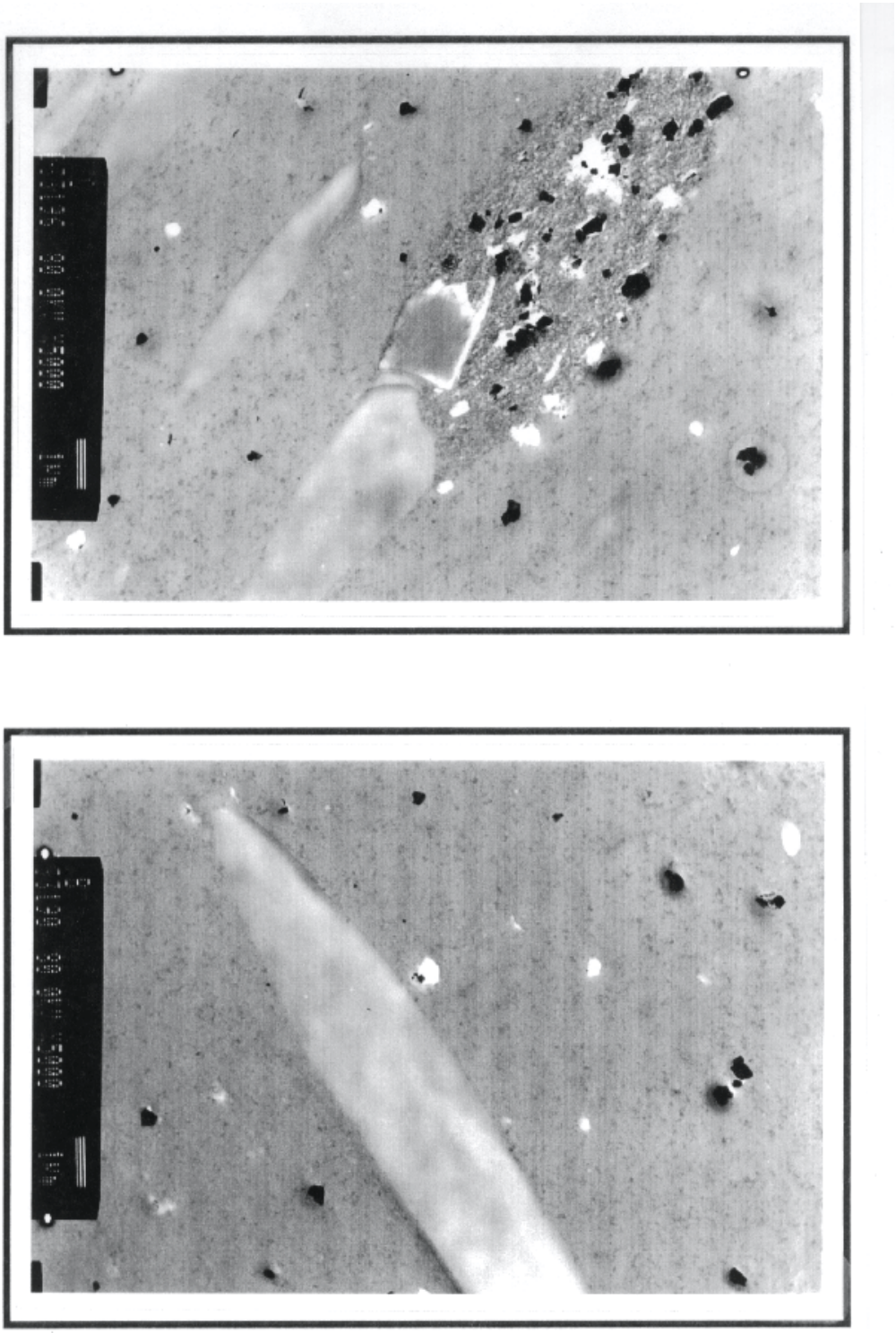

Figure 1. TEM micrographs of toner samples.

where P is the power expended by the extruder and P_0 is the power corresponding to the extruder running empty, i.e., power losses in the drive; efficiency refers to the conversion of electrical energy to mechanical energy in the drive motor. For the extruder used in the experiments of the study, P_0 is about 1 kW and efficiency is 0.9. The measured P values and the specific energy associated with different operating conditions are given in Table II. The mixing intensity increases with increasing rpm or decreasing flow rate.

Table II. Process Parameters and the Associated Specific Energy Values

Screw rpm	Feed rate (kg/h)	Power (P) (kW)	Specific energy (kW-h/kg)
150	1.5	2.0	0.60
150	8.0	2.8	0.20
200	8.0	3.2	0.25
250	8.0	3.8	0.32

The mixing conditions of 150 rpm, 8 kg/h (0.20 kW-h/kg) and 150 rpm, 1.5 kg/h (0.60 kW-h/kg) represent extreme cases, and materials corresponding to those mixing conditions are useful for gross comparisons. Also 150 rpm, 8 kg/h (0.20 kW-h/kg) and 250 rpm, 8 kg/h (0.32 kW-h/kg) represent another set of significantly different mixing conditions.

First the binder was processed without adding any fillers. Next the toner samples were obtained by incorporating all the fillers into the binder. Where appropriate, material analysis was performed with multiple samples for statistical calculation of the averages and plus-or-minus error given by a 95% confidence interval.

Microstructural Characterization

Filler Microstructure

The filler particles used in the formulation are generally submicrometer in size. Transmission electron microscopy was used to obtain micrographs of the material samples at a magnification of 5000×. At this magnification, the dimensions of the view area are 15×10 μm, approximately the cross section of an average size toner particle. Six micrographs corresponding to each processing condition were taken to obtain multiple views.

Figures 1(a) and 1(b) show two micrographs of a typical toner. Large black particles in the micrographs are the magnetite particles, white irregular shapes are the organic pigments, and gray elliptical shapes are the wax particles. The carbon black particles are very small as compared with the other fillers; carbon black appears as dots in the background. Two qualitative observations could be readily derived from the micrographs:

1. There is a tendency of the fillers to be trapped within the gel, i.e., the part of the polymer that is partially crosslinked. [See, for example the filler particles concentrated in the upper right area of Figure 1(a)]. The polymer content is generally selected to adjust the fusing properties of the toner.[9] It is possible to understand from the micrographs that high polymer gel content has a detrimental impact on the dispersion of the fillers.
2. In some cases, the wax fillers exist as large particles several micrometers in length. Considering that the average toner particle is about 10 μm in diameter, the existence of large wax particles suggests that wax distribution within the toner could be very nonuniform.

Particle-size distribution of the wax particles, as well as the other fillers, were characterized in detail to relate these quantities to the processing conditions. The dimensions of the filler particles were measured from the TEM micrographs, using calipers with an accuracy of about ±10 nm in actual dimensions. Particles as seen in the micrographs were approximated as ellipses, and for each particle two measurements were taken: the long axis, a, and the short axis, b. The particle radius, r, and aspect ratio, AR, were calculated from:

$$\pi r^2 = \pi (a/2) \times (b/2), \quad (2)$$

$$\mathrm{AR} = a/b. \quad (3)$$

For the case of rigid fillers like magnetite, measurement of the AR made it possible to calculate the shape distributions in addition to the size distributions. These distributions provide information about the degree of dispersive mixing that the material has undergone.

Magnetite. Figure 2 shows particle size distributions for magnetite. As the specific energy is increased, larger magnetite particles undergo attrition and the particle size distribution becomes narrower. This result can also be observed in the variation of the average particle size with specific energy, as shown in Figure 3. The average size decreases sharply to about half of the original value upon processing. The reduction saturates at about 0.25 kW-h/kg, suggesting that the limit of the dispersion capability might have been reached. Comparison of the size values at 0.20 kW-h/kg (150 rpm, 8 kg/h) and at 0.60 kW-h/kg (150 rpm, 1.5 kg/h) shows a noticeable decrease at the lower feed rate, confirming that lowering of the feed rate increases the intensity of the mixing. AR distributions of magnetite are shown in Figure 4. The mixing process clearly changes the shape of the particles. At the lowest specific energy the particles are mostly round as indicated by the narrowly distributed, low ARs. The distribution broadens from 0.20 to 0.25 kW-h/kg, indicating that the mixing process breaks the particles into more irregular shapes having higher ARs. The change from 0.25 to 0.32 kW-h/kg is not very pronounced. Broadening of the distribution from 0.20 kW-h/kg to 0.60 kW-h/kg is clear. Generally, the trends observed in the AR distributions confirm those observed in the size distributions.

Charge Control Agent. The particle size distributions of the CCA vary only slightly with the mixing conditions. Therefore, only the average size values are shown in Figure 3.

Wax. The temperature of the melt during processing is in the range 135 to 150°C, usually higher than the specified melting temperature of the wax. Hence wax particles exist in the mix in a molten state. This is also evident from the smooth shapes seen in the micrographs. Dispersion of an immiscible fluid in the binder can be expected to be different from that of rigid fillers. The size distributions of the wax particles, given in Figure 5, change with the mixing conditions, but the changes do not correlate with the specific energy. Indeed, at the highest specific energy the particles consist of very large or very small sizes, giving the poorest distribution of the four cases. The narrowest distribution is obtained at the intermediate specific energy of 0.25 kW-h/kg, though particles of micrometer size constitute an appreciable number for that case, too.

Spatial Distribution of the Main Filler. The sizes of most of the carbon black particles in the micrographs were observed to be close to the specified primary particle size, indicating that the dispersive mixing of the main filler was satisfactory. The distribution of the carbon black particles within the binder was investigated from the micrographs. Carbon black appeared as black dots against the gray background of the binder. Sections of the micrographs (about 30 μm^2 each) that contained only carbon black particles were chosen. By using image analysis software, the contribution of the carbon black to the average gray value of the selected area was determined. The average gray level is a measure of the concentration of the carbon black in the binder. Results plotted in Figure 6 show that average

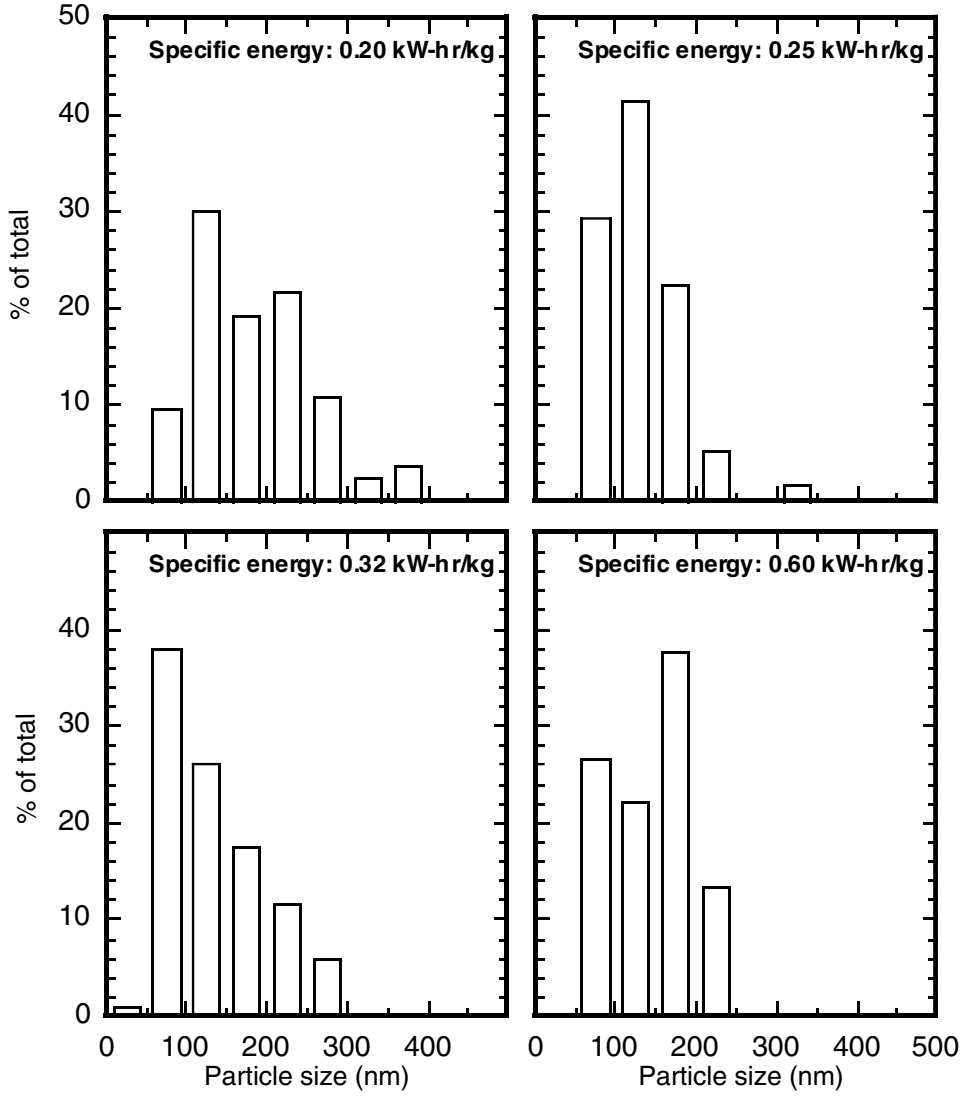

Figure 2. Size distributions of magnetite particles for different mixing conditions.

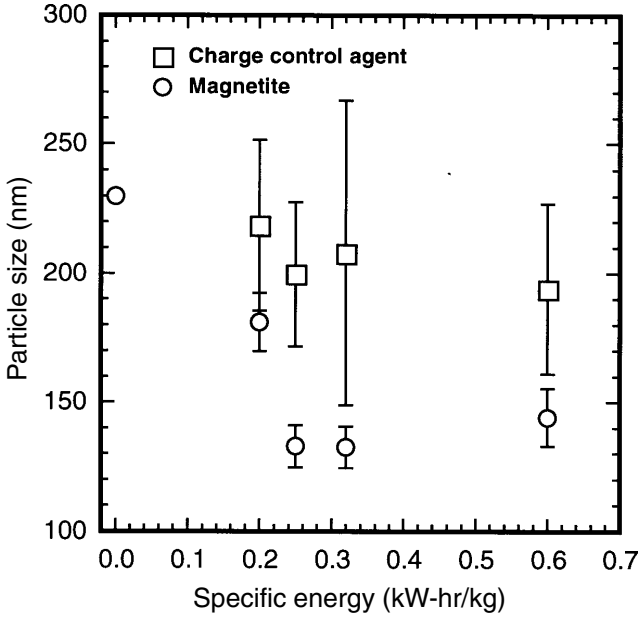

Figure 3. Variation of the average particle size values of the minor fillers with mixing conditions.

gray values are about the same for all the mixing conditions, as expected. The sizes of the error bars, which are proportional to the standard deviation of the gray levels of different regions, give information about the homogeneity of the distribution. The distribution is most nonuniform at the lowest specific energy. The uniformity does not improve with increasing specific energy. The smallest error bars are obtained at the intermediate energy value of 0.25 kW-h/kg. This result, similar to the result obtained with the size distribution of the wax particles, indicates that the distributive mixing of the fillers does not scale with the specific energy.

Binder Microstructure. ***Molecular Weight Distributions of the Polymer***. One of the significant issues is the possibility that binder microstructure might change during the twin-screw extrusion. Conditions of high shear deliberately employed to disperse the additives are known to cause deleterious effects in terms of lowering the molecular weight and broadening the molecular weight distribution (MWD).[10] Changes in the microstructure affect the physical properties of the toner and have a bearing on the printing performance. Gel permeation chromatography (GPC) was used to characterize the MWDs of the binder polymer. The instrument employed for the GPC experiments was a Tosoh

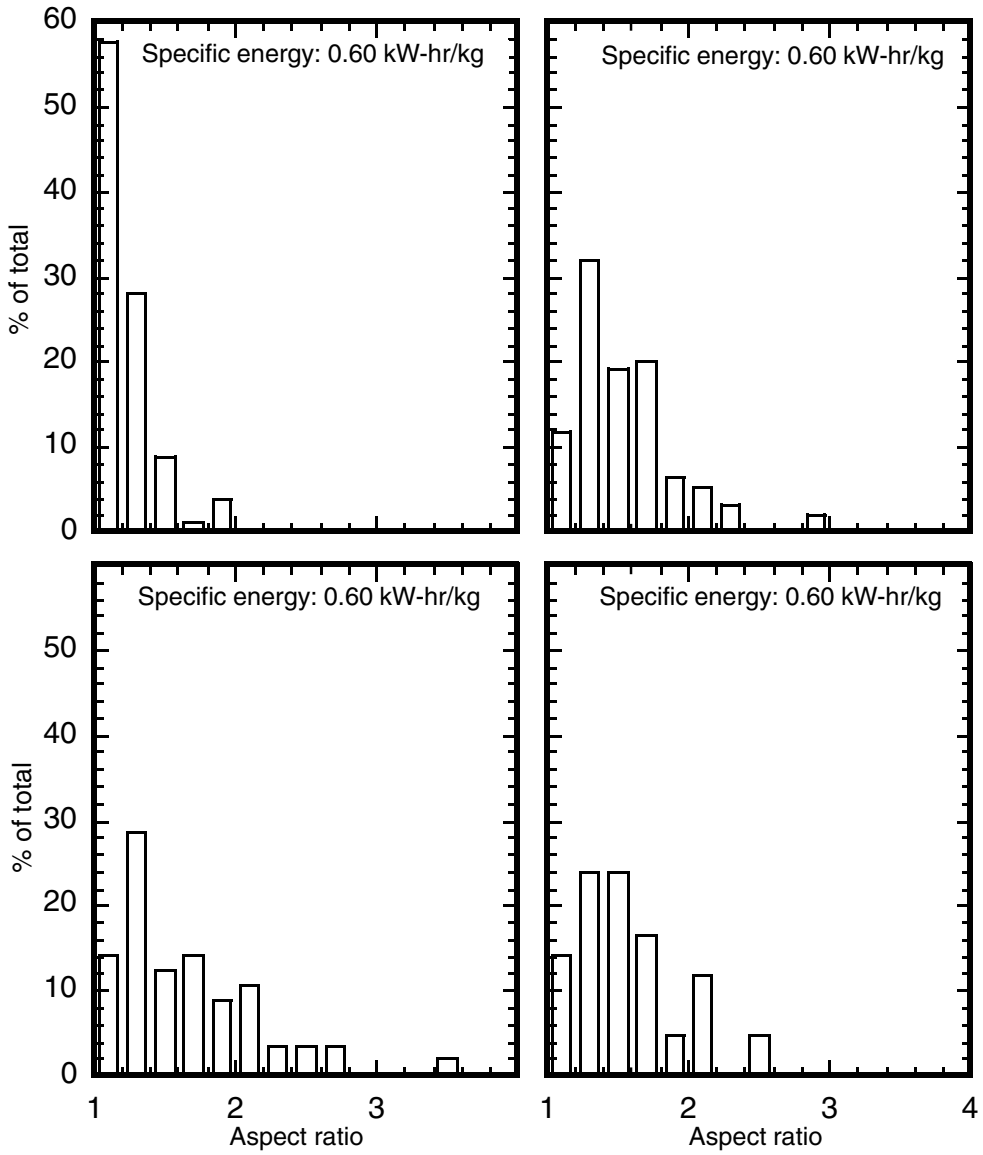

Figure 4. AR distributions of magnetite particles.

Model SC-8020 equipped with a column GMHXL + G300HXL. Material samples dissolved in chloroform (5 g/L) were circulated through the column at a rate of 1 mL/min at 28 kgf/cm^2 pressure. The temperature of the solution was kept at 40°C during the experiment. Polystyrene served as a reference sample for the MWD calculations.

The calculated MWDs of the "binder only" samples are shown in Figure 7. Three observations can be obtained from this result:

1. Processing of the binder gives rise to substantial increases in the molecular weights in the range 10^5 to 10^7 as compared with that of the unprocessed binder (B-0).
2. This increase is particularly pronounced for the binder processed at the highest specific energy, 0.60 kW-h/kg.
3. Molecular weight distributions of the binder samples corresponding to 0.20, 0.25, and 0.32 kW-h/kg are only slightly different from one another.

MWDs of the toner samples have features similar to those of the binder-only data.

The results of the GPC experiments suggest that most of the changes in the binder microstructure occur in the gel part of the binder. The MWDs corresponding to the gel of the unprocessed polymer do not appear in the GPC results, because the gel does not dissolve in the chloroform solution and it is filtered out. In the case of the processed material, the mixing action alters the structure of the gel by breaking some of the partial crosslinks. Damaged gel molecules become soluble in the chloroform solution, and they are detected by the GPC as large molecular weight components of the polymer.

Softening Temperature Measurements. Softening temperature, T_{sp}, of the material serves as an indicator of the microstructural changes in the binder. Measurements of T_{sp} were carried out using a Model CFT-500 flow tester (Shimadzu). Results of the softening temperature measurements are summarized in Fig. 8. The softening temperatures of the processed binders are very different from that of the

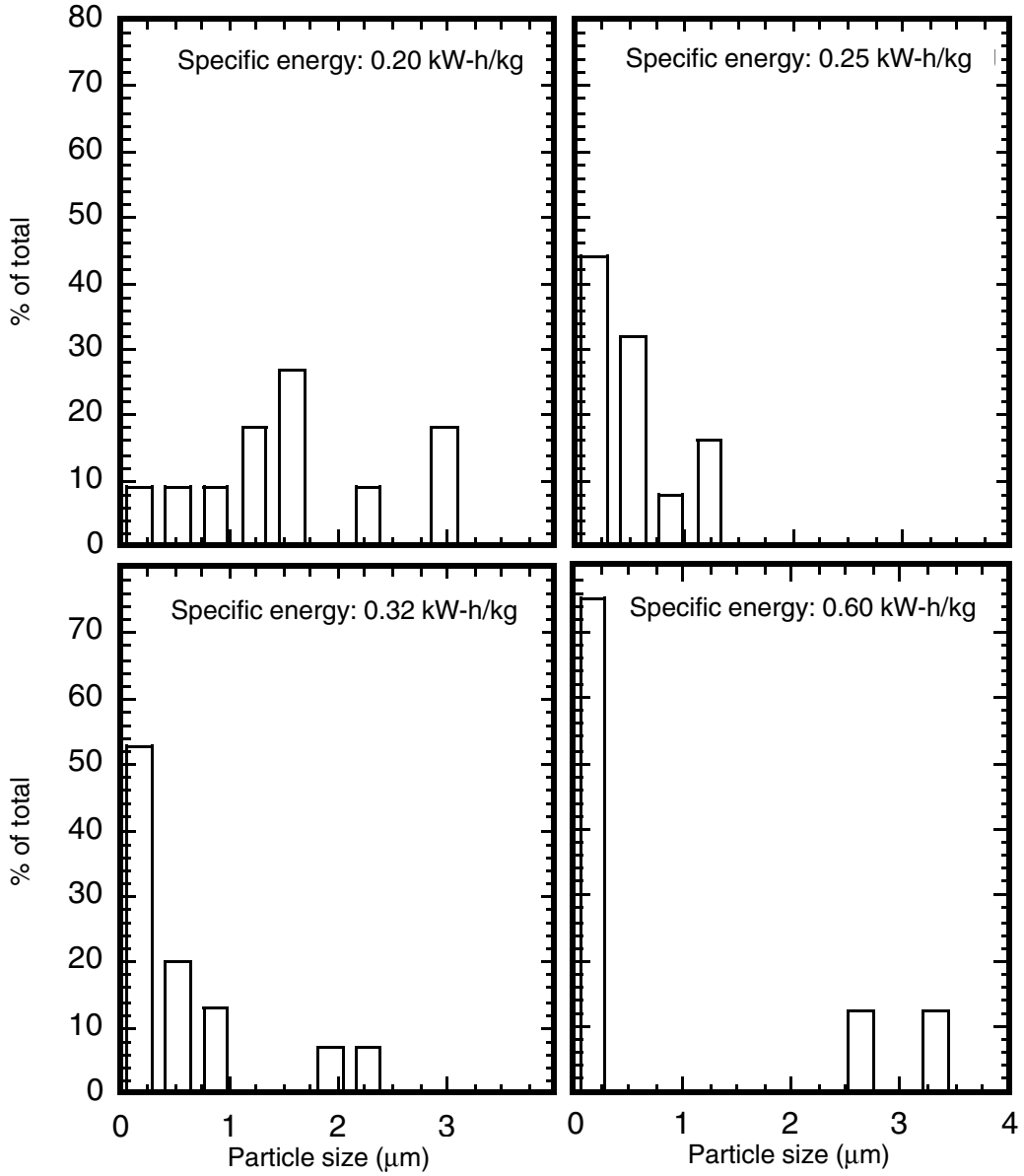

Figure 5. Size distributions of wax particles for different mixing conditions.

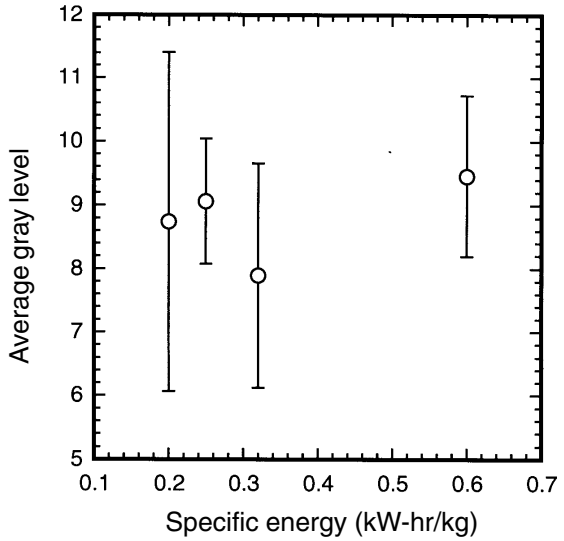

Figure 6. Gray value contribution of carbon black particles as an indicator of the homogeneity of their spatial distribution.

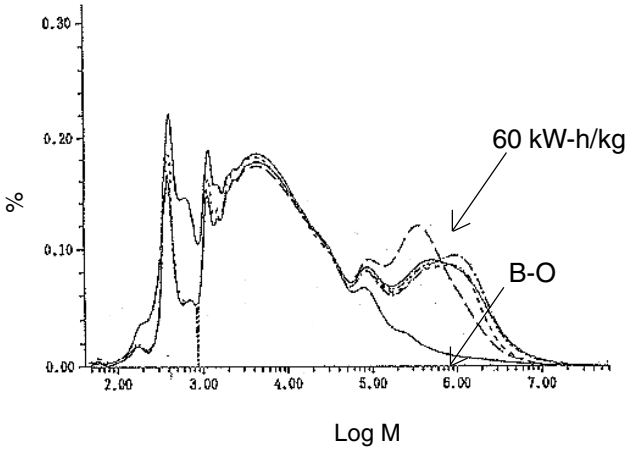

Figure 7. Molecular weight distribution of the binder samples; B-0 is the unprocessed binder for comparison.

unprocessed reference shown at zero energy. The binder samples corresponding to the lowest three specific energies have similar softening temperatures. The softening temperature of the binder processed at the highest specific energy is the lowest, indicating a distinction in the microstructure compared with the other processed binders. Toner results are qualitatively the same as the binder results. The trends concur with the findings obtained with the GPC experiments.

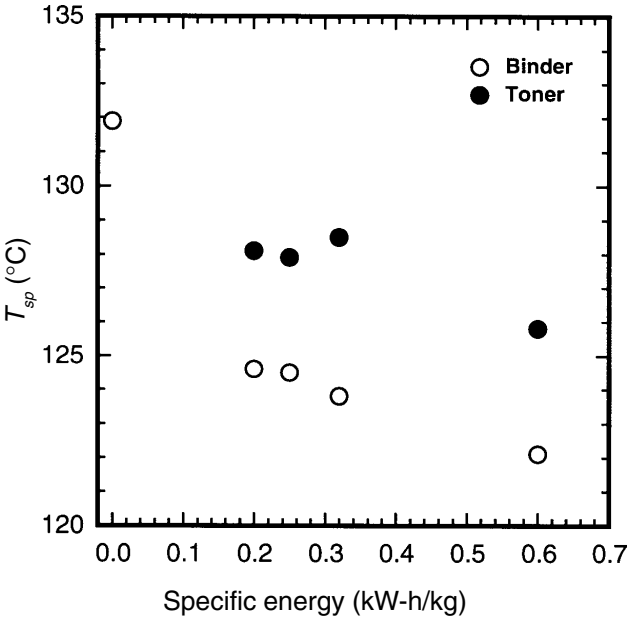

Figure 8. Softening temperature results.

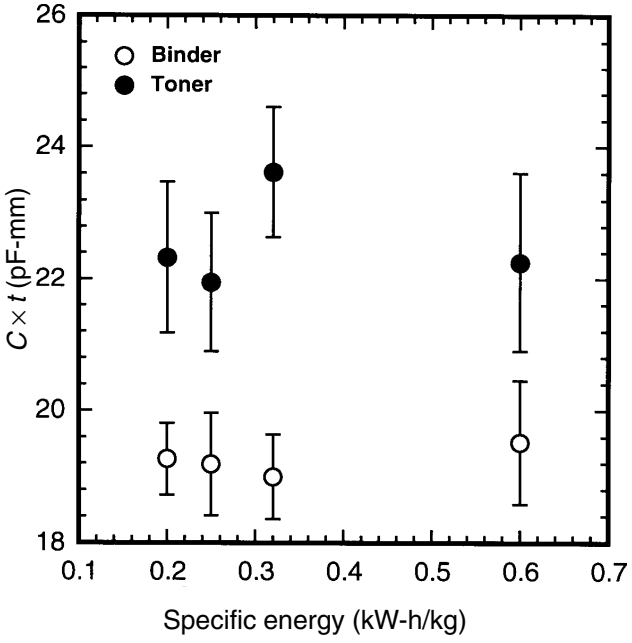

Figure 9. Polarizability of the binder and the toner samples at room temperature; measurement frequency: 1kHz.

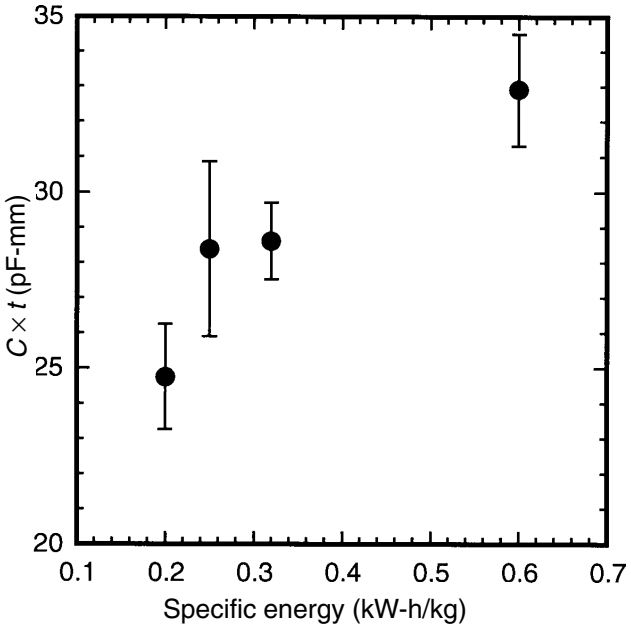

Figure 10. Polarizability of the toner samples at 150°C; measurement frequency: 1 kHz.

Macroscopic Characterization

Temperature-Variable Dielectric Measurements.

The volume fraction of the fillers in the composite is relatively small, overall less than about 10% by volume. Therefore it is more appropriate to focus on the dielectric properties of the binder. At temperatures above the glass transition temperature, segmental motion of the side groups attached to the main polymer chain becomes possible. Above the softening temperature the polymer chains are able to move as a whole. Attainment of such spatial degrees of freedom gives rise to the enhancement of the dielectric properties of polar polymers like the polyesters.[11] For this reason, dielectric properties are more interesting at elevated temperatures than at room temperature.

Temperature-variable dielectric measurements were performed utilizing a rheometer setup. A Dynamic Analyzer II rheometer (Rheometrics) with parallel plate disposable fixtures was modified so that electrical connections could be made to samples equipped with metal electrodes. The oven of the rheometer enabled measurements over a broad range of temperatures. The temperature was increased in three steps of 85, 120, and 150°C. The measurements were performed by using an impedance analyzer, Model HP4192A. The dimensions of the samples were diameter of 25 mm and thickness of 1.5 to 2 mm.

The electrical model of the capacitor formed by metal electrodes and the material sample consist of an ideal capacitor, C, in parallel with an ideal resistor, R. The polarizability of the material is reflected in the capacitance, and the charge mobility in an alternating field is reflected in the conductance, G, of the resistor. The values of C and G measured by the impedance analyzer can be related to the material properties dielectric constant K, conductivity s, and geometric parameters of thickness t and surface area A as follows:

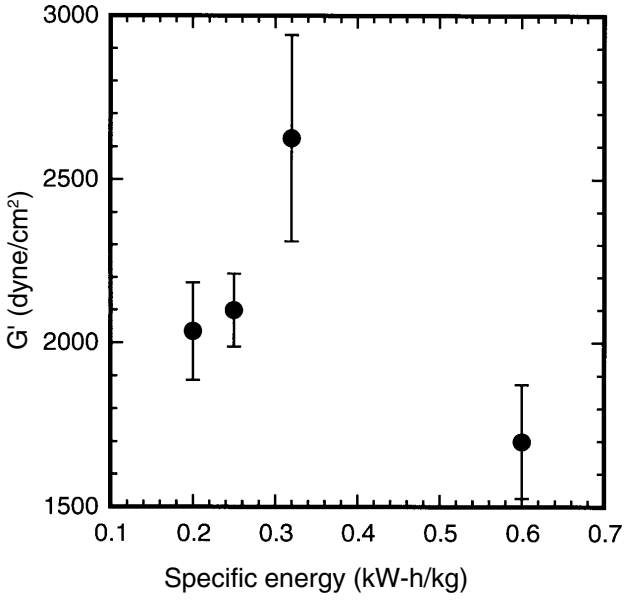

Figure 11. Elasticity of the toner samples at 150°C; measurement frequency: 0.16 rad/s and strain: 50%.

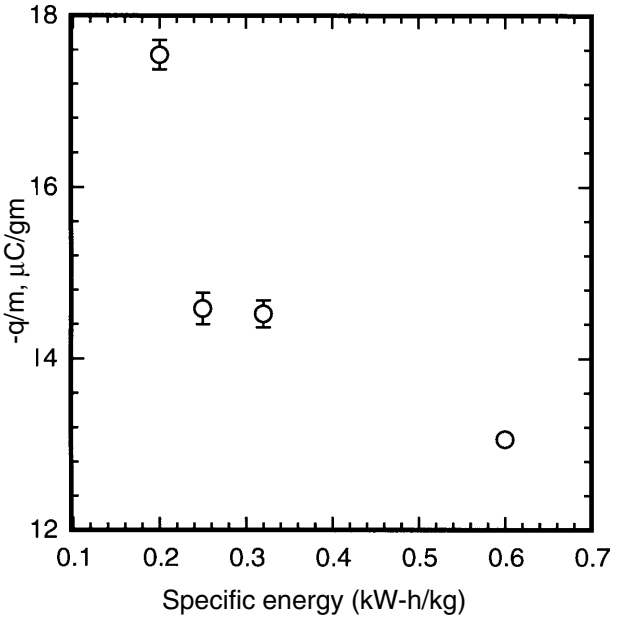

Figure 12. Charge per unit mass values of the pulverized toner samples.

$$C = \frac{K\varepsilon_0 A}{t}, \quad G = \frac{\sigma A}{t}. \tag{4}$$

The measured results were expressed as $C \times t$, which is proportional to the dielectric constant and $G \times t$, which is proportional to the conductivity; A is the same for all samples. Comparison of samples processed under different conditions was emphasized, rather than calculation of the absolute values of K and σ.

Polarizability at Room Temperature. The results of the polarizability measurements performed at room temperature are plotted in Figure 9 as functions of the specific energy. For the binder samples, the $C \times t$ product is the same at all specific energies. In the case of the toner, the average values vary somewhat, but trends are not noticeable. It is difficult to distinguish among the samples processed under different conditions on the basis of room temperature dielectric data.

Polarizability at Processing Temperature. Results of the toner polarizability measurements at 150°C are shown in Figure 10. The polarizability exhibits a generally increasing trend with increasing intensity of mixing. This increase is partially due to changes in the filler microstructure. However, the fact that similar trends are not observable at room temperature suggests that changes in the binder microstructure and binder–filler surface interactions play a major role.

The trends in the conductivity results at 150°C are very similar to those of the polarizability results.

Rheological Measurements. Rheological measurements of the material samples were performed to check their suitability to understand the state of the mix. The experiments were performed with the Dynamic Analyzer II rheometer in conjunction with parallel plate fixtures. The gap height was set at 1.5 mm for all the samples. Oscillatory deformation was applied to the samples at 50% strain while the frequency was swept from 10 to 0.1 s^{-1}, taking five data points per decade. All measurements were carried out at 150°C.

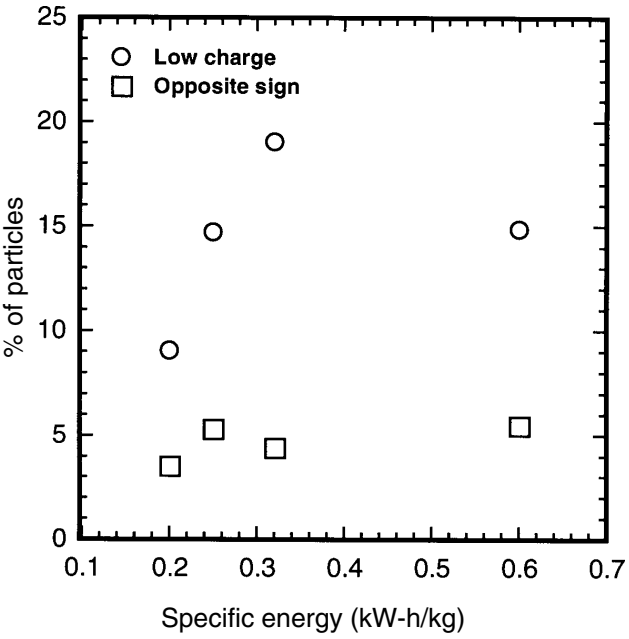

Figure 13. Undesirable charging characteristics of the pulverized toner samples.

Elastic Properties. In the oscillatory measurements, the elastic properties are reflected in the storage modulus, G'. Figure 11 shows the variation of G' as a function of the specific energy for the toner samples. The samples corresponding to the first three specific energies show an increasing trend of elasticity with increasing intensity of mixing. This result is due to the reinforcing effect of the carbon black, which is well known in the rubber industry.[12,13] The structured and chemically active carbon black surface is believed to function as a crosslinking agent; polymer molecules become physisorbed or chemisorbed onto the surfaces of the particles. Toner samples processed at higher

mixing intensities have a greater carbon black surface area due to the attrition of the fillers. Therefore, the surface interaction and the elasticity increase with increasing energy. At the highest specific energy, the elasticity drops sharply. This drop may be associated with a significantly different binder microstructure.

The viscous properties as given by the loss modulus, G'', exhibit trends very similar to those of the elastic properties.

Charging Properties. The macroscopic measurements explained above used bulk material samples obtained after twin-screw extruder processing. To investigate the charging properties, bulk samples were further processed to obtain pulverized powder. The pulverization involved grinding of the samples to an average diameter of about 14 μm in a supersonic jet mill and eliminating the particles less than 5 μm in diameter in a classifier. The size-sorted powder was mixed with fumed silica to improve the flow properties and then blended with a silicon-coated ferrite carrier of 100 μm diameter in proportions of 97 to 3 by weight.

The charge per unit mass, q/m, of the toner/developer mixture was measured by the blow-off method, which employed a Faraday-cage-based instrument built in house. The charge per unit mass values of the material samples processed under different conditions are plotted in Fig. 12. The data show a generally decreasing trend of q/m with increasing intensity of the mixing, i.e., increasing rpm and decreasing feed rate. The q/m values for 0.25 and 0.32 kW-h/kg are about the same.

The charge/diameter, q/d, distributions of the toner particles were characterized by a particle-charge spectrum analyzer. The distribution exhibits a double peak structure, the smaller peak occurring at the lower charge range. Differences in the processing conditions give rise to changes in this secondary distribution. The area and the peak value of the secondary distribution grow with more intensive mixing. The fractions of particles having the wrong sign charge and low charge, defined as $q/d < 0.2$ fC/μm, are calculated from the distributions. The results of these undesirable charging characteristics are plotted as functions of the specific energy in Fig. 13. The fraction of particles bearing low charge increases with mixing intensity. Changes in the fraction of particles bearing the wrong sign charge are less pronounced. The sample processed at 0.60 kW-h/kg has a greater number of particles with the wrong sign charge than does the one processed at 0.20 kW-h/kg.

Overall, the results indicate that charging properties are adversely affected by increasing intensity of mixing.

Conclusions

- Distributive mixing of the main filler does not improve with increasing specific energy. Ways of improving the homogeneity of the filler distribution need to be studied in conjunction with different screw configurations.
- High gel content is detrimental to good mixing. Trapping of the filler particles within the gel regions might be tolerable up to a certain gel concentration, but from the point of view of mixing, a homogeneous, "gelless" binder is more desirable.
- Particle size and shape distributions of the fillers are affected differently by the mixing conditions. In the case of magnetite, the size distribution becomes narrower with increasing energy, whereas for wax it broadens.
- The binder molecular weight distributions change significantly during processing, even at the lowest specific energy used in the experiments. The mixing mostly affects the microstructure of the gel.
- Changes in the mixing conditions of the toner can be observed in the dielectric properties measured at the processing temperature. This result is promising for monitoring the state of the mix on-line.
- Rheological properties of the toner are also sensitive to the mixing conditions and might be utilized as on-line monitoring tools.
- Charging properties of the toner are adversely affected by increasing intensity of mixing, as illustrated by lower q/m values and poorer charge distributions.

Acknowledgments

The authors would like to thank Mr. Sonobe, Mr. Maeda, Ms. Ueno, Ms. Ikeda, and Ms. Makino of Kao research laboratories for their assistance with various aspects of the experimental work. The authors would also like to thank Dr. Maki and Mr. Ueda of Kao Research Labs for reviewing the manuscript and making useful suggestions. One of the authors (H. G.) would like to express his gratitude to Kao Corporation for the visiting appointment provided at the Kao Recording and Imaging Science Laboratories.

References

1. G. P. Marshall, Current trends in dry toner technology, Tutorial Notes, *Proceedings of IS&T's 10th International Congress on Advances in Non-Impact Printing Technologies,* 1994.
2. D. M. Kalyon, Mixing in continuous processors, in *Encyclopedia of Fluid Mechanics*, Vol. **7**, N. Cheremisinoff, Ed., Gulf Publishing Company, Houston, 1988, p. 887.
3. J. L. White, *Twin Screw Extrusion*, Hanser Publishers, Munich, 1991.
4. L. B. Schein, *Electrophotography and Development Physics*, Springer-Verlag, Berlin, 1988.
5. E. M. Williams, *The Physics and Technology of Xerographic Processes*, John Wiley, New York, 1984.
6. T. Satoh, T. Kawanishi, R.Shimizu, and N. Kinjo, Rheological study on fixing polyester resin toners, *J. Imaging Sci.* **35**: 373 (1991).
7. A. Stübbe and W. Schumacher, Pigment blacks in toners for electrophotographic copying process, *Am. Ink Maker* **65**: 18 (1987).
8. C. J. Rauwendaal, Analysis and experimental evaluation of twin screw extruders, *Polym. Eng. Sci.* **21**: 1092 (1981).
9. T. E. Karis, C. M. Seymour and M. S. Jhon, The coupled relaxation model for toner melt rheology, *Polym. Eng. Sci.* **31**: 99 (1991).
10. P. R. Hornsby and G. R. Sothern, Polymer degradation during twin screw extrusion compounding, *Plastics and Rubber Proc. Appl.* **4**: 165 (1984).
11. J. A. Brydson, *Plastic Materials*, 5th Ed., Butterworth, Boston, 1989.
12. D. H. Morton-Jones, *Polymer Processing*, Chapman and Hall, London, 1989.
13. K. Lakdawala and R. Salovey, Viscosity of copolymers containing carbon black, *Polym. Eng. Sci.* **25**: 797 (1985).